

# Dynamic mechanical and dielectric relaxation in a series of main chain thermotropic liquid crystalline polyesters

Peter Avakian, John C. Coburn, Mark S. Connolly and Bryan B. Sauer\*

DuPont Central Research and Development, Science and Engineering Laboratories,  
 Wilmington, DE 19880-0356, USA

(Received 6 May 1995; revised 4 January 1996)

The effects of structural changes on the frequency dependent dynamic mechanical (d.m.a.) and dielectric relaxation behaviour in a series of wholly aromatic thermotropic main chain liquid crystalline (LC) polyesters were investigated. The polymers were side-group substituted poly(hydroquinone-terephthalates), modified with biphenols and 4-hydroxybenzoic acid. The side groups, R, were varied as R = methyl, phenyl, or t-butyl. Data were also obtained for Vectra A950. These LC polymers exhibit three prominent relaxation processes. Some of the LC polymers in this series are 'non-crystalline' with strong and narrow glass transitions which are shown to vary as much as 80°C depending on the choice of substitution of the hydroquinone group. Tertiary butyl substitution on the hydroquinone units was found to lead to the highest glass transition (*ca* 185°C). Another common feature of most of these LCPs is a sharp but weak second 'glass transition' observed at lower temperatures than the main glass transition. This is attributed to motions of non-substituted aromatic ester species including 4-hydroxybenzoic acid (HBA) due to their relatively low barriers to rotation. Comparisons are made with the wholly aromatic, HBA-rich, LC polymer, Vectra<sup>®</sup>. Three of the LC polymers exhibit essentially the same subglass  $\gamma$  relaxation at *ca* 60°C (1Hz) which is attributed to local motion involving the non-substituted aromatic units such as HBA. Adding methyl side group substituents to the *ortho* position of the biphenol group restricts the subglass  $\gamma$  process in a kinetic sense, shifting the process to higher temperatures. The effect of substitution of the hydroquinone group on the  $\gamma$  relaxation was also systematically investigated. Copyright © 1996 Elsevier Science Ltd.

(Keywords: liquid crystalline polymer; dielectric; mechanical; relaxation; glass transition)

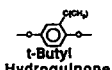
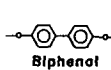
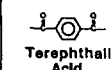
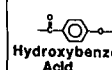
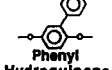
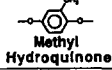
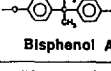
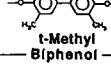
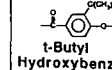
## INTRODUCTION

Thermotropic liquid crystalline (LC) polymers have received much attention as engineering resins<sup>1–10</sup>. These polymers have high use temperatures and the mesomorphic melt is highly shear sensitive resulting in low melt processing viscosities<sup>2,8,11</sup> and moulded parts with highly anisotropic mechanical properties resulting from preferential molecular chain axis alignment. Several companies including Hoechst-Celanese, Amoco, and DuPont have marketed thermotropic LC polymers. The most basic structure of liquid crystalline polyesters, *p*-phenylene groups connected by ester groups, is highly crystalline in the solid state with very high melting temperatures (> 400°C), well above their degradation point or too high for conventional melt processing equipment, making these materials commercially impractical. Several approaches, have been reported<sup>2–8</sup> to reduce the melting point of these polymers. These approaches include introducing flexible aliphatic spacers, adding side group substituents to the main chain, modifying the regular structure of the main chain with comonomers, and/or introducing rigid kinks into the linear polymer chain.

Relaxation studies on main-chain liquid crystalline polymers reported in the literature have generally focused on liquid crystalline polymers with flexible methylene segments along the polymer backbone<sup>12–16</sup>. Interpretation of the results of these studies have been complicated by overlap of relaxation processes of the flexible and stiff components. Several studies have focused on the relaxation behaviour in liquid crystalline copolyesters with more 'rigid' comonomers that are semi-crystalline in the solid state<sup>8,17–25</sup> such as Hoechst-Celanese's Vectra<sup>®</sup>. Here we report on the dielectric and mechanical relaxation behaviour of a series of high glass transition ( $T_g$ ), wholly aromatic thermotropic liquid crystalline polyesters based on substituted hydroquinones, 4,4'-biphenol, terephthalic acid, and 4-hydroxybenzoic acid (HBA). For three of the LC polymers, different substituted hydroquinones are used. In two cases biphenol is replaced and in the final case a substituted hydroxybenzoic acid replaces HBA (*Figure 1*). This series is composed entirely of aromatic segments along the backbone as is the case for Vectra<sup>®</sup> which is included in the frequency dependent dynamic mechanical (d.m.a.) part of this study.

Because of sufficiently disrupted chain structure, some of the copolyester LC polymers in this series exhibit unique behaviour in that they have no detectable

\*To whom correspondence should be addressed

LIQUID CRYSTALLINE POLYESTERS				
LC1	 t-Butyl Hydroquinone	 Biphenol	 Terephthalic Acid	 Hydroxybenzoic Acid
LC2	 Phenyl Hydroquinone			
LC3	 Methyl Hydroquinone			
LC4		 Bisphenol A		
LC5		 t-Methyl Biphenol		
LC7				 t-Butyl Hydroxybenzoic Acid

**Figure 1** Schematic of the series of liquid crystalline polymers used in this study. The 'control' polymer, LC1, was prepared from the four units indicated: t-butyl hydroquinone/4,4'-biphenyl/terephthalic acid/HBA in the ratio 80:20:100:100, respectively. The 80:20:100:100 ratio is kept constant for the others in the figure, but the indicated monomers are substituted for their respective counterparts in the control LC1

three-dimensional or crystalline order. The polyesters that do not undergo a liquid crystalline to crystalline transition, exhibit prominent glass transitions. Above  $T_g$ , these polymers exhibit liquid crystalline behaviour. Below  $T_g$ , the nematic ordering is essentially frozen-in.

## EXPERIMENTAL

### Synthesis

Vectra<sup>®</sup> A950 (Hoechst-Celanese) is a copolyester consisting essentially of 73% HBA and 27% hydroxy naphtholic acid (HNA). The rest of the series of liquid crystalline polymers used in this study are shown schematically in *Figure 1*. The base polymer, LC1, was prepared from the four substituents of t-butylhydroquinone, 4,4'-biphenol, terephthalic acid and 4-hydroxybenzoic acid in mole ratios of 80:20:100:100, respectively. The effect of different substituents on the hydroquinone (LC2, LC3) and 4-hydroxybenzoic acid (LC7) groups was studied, as well as the effect of substituting for the 4,4'-biphenol group (LC4, LC5). All polymers in the series contain the same molar ratios of aromatic diol, aromatic dicarboxylic acids, and aromatic hydroxybenzoic acid, i.e. 80:20:100:100 (*Figure 1*).

Standard solvents and aromatic diacids [terephthalic (T) acid] were obtained from DuPont Chemicals and were used as received. Acetic anhydride (Fisher, ACS Grade) was used as received. Many of the aromatic hydroxycarboxylic acids, dicarboxylic acids, and 'polyaromatic diols' are available in commercial or developmental quantities from UENO Fine Chemical, Aldrich, Amoco, or Eastman Chemical.

The polymers were prepared by a standard melt polymerization process. The copolyesters were prepared from the diacetates of hydroquinones and acetates of hydroxycarboxylic acids. The dicarboxylic acids were used as such rather than as esters or other derivatives. The acetate analogues were either added directly to the

resin kettle or were generated *in situ*. The monomer ingredients were added in substantially the same molar ratios as desired in the final polymer except that an excess (usually 0.5 mol%) of the major hydroquinone component was used.

*Acetylation of aromatic diols, general procedure.* The aromatic diols and hydroxycarboxylic acids were allowed to react with acetic anhydride in a similar manner. The following procedures are typical. (a) Acetic anhydride (11, 9.05 mol) was added to a flask equipped with a 'Drierite' drying tower and containing t-butylhydroquinone (500 g, 3.01 mol). Two drops of sulfuric acid catalyst were added. The solution was stirred at room temperature for 10 min, then heated slowly over 1 h to reflux. It was maintained at reflux for 1 h. After that time, the solution was allowed to cool to room temperature overnight. The product was purified by precipitation into iced water (2.5 l), was collected by filtration under reduced pressure, washed with distilled water (1 l) and dried overnight in a vacuum oven (45°C, 17–20 in. Hg) with a nitrogen purge. It was recovered as a fine white powder (765.1 g, 97%). (b) Acetic anhydride (850 ml, 9.0 mol) was added to a flask equipped with a 'Drierite' drying tower and containing HBA (610.4 g, 4.42 mol) and 2 drops of sulfuric acid catalyst was added. The solution was heated slowly and maintained at reflux for 3 h. After this time, the solution was allowed to cool until all bubbling had stopped and was poured slowly into iced water (2 l). The product was isolated as described above, but was not washed with methanol. A white powder (704.2 g, 90.5%, d.s.c. m.p. 192.0°C) was recovered after drying.

*Polymerization, general procedure.* A resin kettle (0.5 l) was fitted with (1) a stainless steel stirrer extending through a pressure-tight PTFE bushing, (2) a nitrogen inlet, and (3) a short column leading to a water-cooled condenser with a receiver for collecting acetic acid by-product. An attachment for application of vacuum was also provided. An electrically heated Alloy 281 bath, mounted for vertical adjustment, was used for heating. The reaction mixture was heated to increasing temperatures with stirring at atmospheric pressure under a nitrogen purge until at least 85% of the theoretical acetic acid had evolved. The vacuum was then applied and pressure gradually reduced from atmospheric to less than 1 mm Hg. Heating under vacuum at approximately 0.05 mm Hg was continued until the viscosity had increased to acceptable levels. The polymer was removed from the resin kettle while hot, cooled to room temperature and comminuted.

### Methods

The inherent viscosity, a measure of molecular weight, was computed from  $\eta_{inh} = (\ln \eta_{rel}/C)$ , where  $\eta_{rel}$  is the relative viscosity and  $C$  is the solution concentration in grams of polymer per decilitre of solvent. Relative viscosity,  $\eta_{rel}$ , is the ratio of the polymer solution flow time to solvent flow time in a capillary viscometer (e.g., Cannon #E137-100) at 30°C. The solvent mixture employed consisted of 50:50 by volume of 1,2-dichloroethane and 4-chlorophenol. The inherent viscosities of the resulting polymers are reported in *Table 1*.

Densities were determined using a density gradient column at room temperature.

**Table 1** Physical and thermal properties of the LC polymers

Sample	Description <sup>a</sup>	I.V.	Density (20°C) (g cm <sup>-3</sup> )	T <sub>g</sub> (°C)	T <sub>m</sub> (°C)	ΔH <sub>m</sub> (kJ g <sup>-1</sup> )
LC1	t-BuHQ/BP/T/HBA	3.42	1.29	185		
LC2	Ph-HQ/BP/T/HBA	3.45	1.34	157		
LC3	Me-HQ/BP/T/HBA	nd	1.36	100	300	10
LC4	t-Bu-HQ/BPA/T/HBA	1.82	1.27	183		
LC5	t-Bu-HQ/t-Me-BP/T/HBA	5.13	1.27	185		
LC7	t-Bu-HQ/BP/T/t-Bu-HBA	1.93	1.24	172		

<sup>a</sup> See Figure 1 for chemical repeat units

Optical anisotropy was seen in all of these polymers by cross-polarized light transmission through the polymers heated to temperatures above their flow temperatures using a microscope hot stage.

Thermal characterization of the polymers by d.s.c. was performed with the use of a DuPont Model 2100 Thermal Analyzer from room temperature to 400°C at a rate of 10°C min<sup>-1</sup>. A known weight of polymer (usually 5–8 mg) was sealed in an aluminium d.s.c. pan and maintained under nitrogen throughout the test. The sample was then subjected to a heating cycle to remove the effects of prior thermal history. This cycle generally consisted of heating the sample at 10°C min<sup>-1</sup> to 400°C, followed by rapid cooling to room temperature, followed by a second heat-up cycle to 400°C. The glass transition temperature was defined from the midpoint of the change in heat flow from the heat flow *versus* temperature curve measured from the second heat. The crystalline melting temperature (*T*<sub>m</sub>) was defined as the maximum of the crystalline melting endotherm and was measured from the second heat cycle. The heat of fusion was calculated from the area of the crystalline melting endotherm.

D.m.a. data were obtained on DuPont Instruments DMA 983. The frequency range used was 0.1–8 Hz.

The dielectric experiments were carried out with the parallel-plate geometry. The gold–palladium electrodes were sputtered onto the polymer film samples. A Hewlett Packard LCR meter (Model 4274A) was used to measure the capacitance, *C*, and dissipation factor ( $\tan \delta = \epsilon''/\epsilon'$ ) of the sample at 11 frequencies in the range 10<sup>2</sup>–10<sup>5</sup> Hz from –190° to 250°C at a heating rate of 1.5°C min<sup>-1</sup>. A custom-made variable temperature dielectric cell was employed. The data were stored in a Hewlett Packard personal computer. The real  $\epsilon'$  and imaginary  $\epsilon''$  components of the dielectric constant (or dielectric permittivity) were calculated by using

$$\epsilon' = Cd/(\epsilon_0 A)$$

$$\text{and } \epsilon'' = \epsilon' \tan \delta$$

where *d* is the sample thickness,  $\epsilon_0$  the permittivity of vacuum ( $8.854 \times 10^{-12}$  F m<sup>-1</sup>), *A* the metallized electrode area (350 m<sup>2</sup>), and  $\delta$  the loss angle. Comparisons between the dielectric behaviour of different polymers were made at 1 kHz frequency.

## RESULTS

The inherent viscosities, densities, glass transitions and/or melting temperatures and heats of transition are

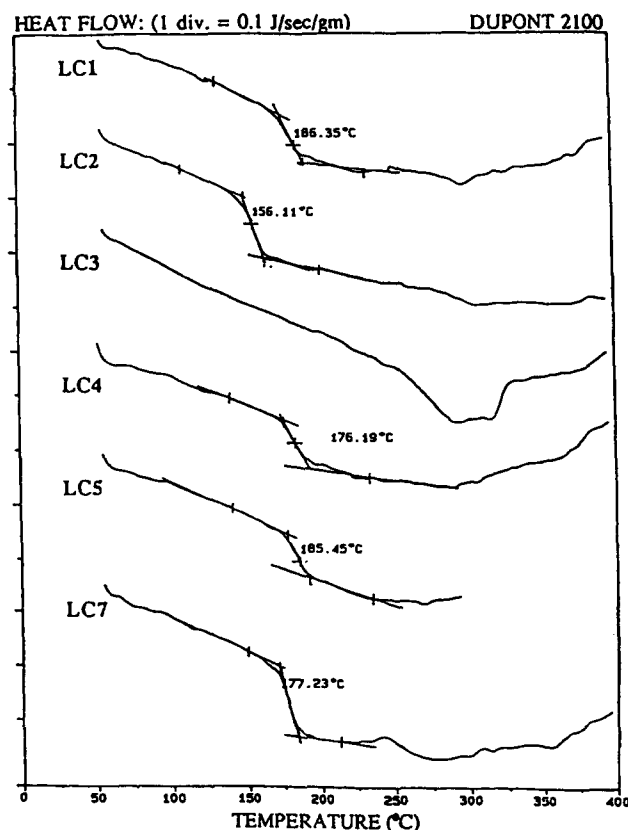


**Figure 2** D.s.c. heat flow *versus* temperature for the six LC polymers studied here

reported in Table 1. D.s.c. heat flow *versus* temperature scans are shown in Figure 2. With the exception of LC3, these polyesters have prominent glass transitions. LC3 has no discernible glass transition by d.s.c. and exhibits a broad and weak melting endotherm around *T*<sub>m</sub> = 300°C. The polyester containing phenyl substituted hydroquinone moiety has a relatively low *T*<sub>g</sub> of 156°C. D.m.a. data presented below for LC3 indicate a much lower *T*<sub>g</sub> than 156°C for that material. The remaining polyesters have approximately equivalent *T*<sub>g</sub>s around 185°C. The *T*<sub>g</sub> of 185°C is one of the highest reported for thermotropic main-chain liquid crystalline polyesters. For comparison, Vectra A950 has a *T*<sub>g</sub> around 100°C even though it is semi-crystalline<sup>18</sup>. *T*<sub>g</sub> varies with substitution on the hydroquinone group in the order t-butyl(LC1) > phenyl(LC2) > methyl(LC3) (see also Figure 1). Literature data for a chloro-substituted hydroquinone-containing analogue of LC1 show a clear *T*<sub>g</sub> of 110°C. The trend in *T*<sub>g</sub>s can be explained by the

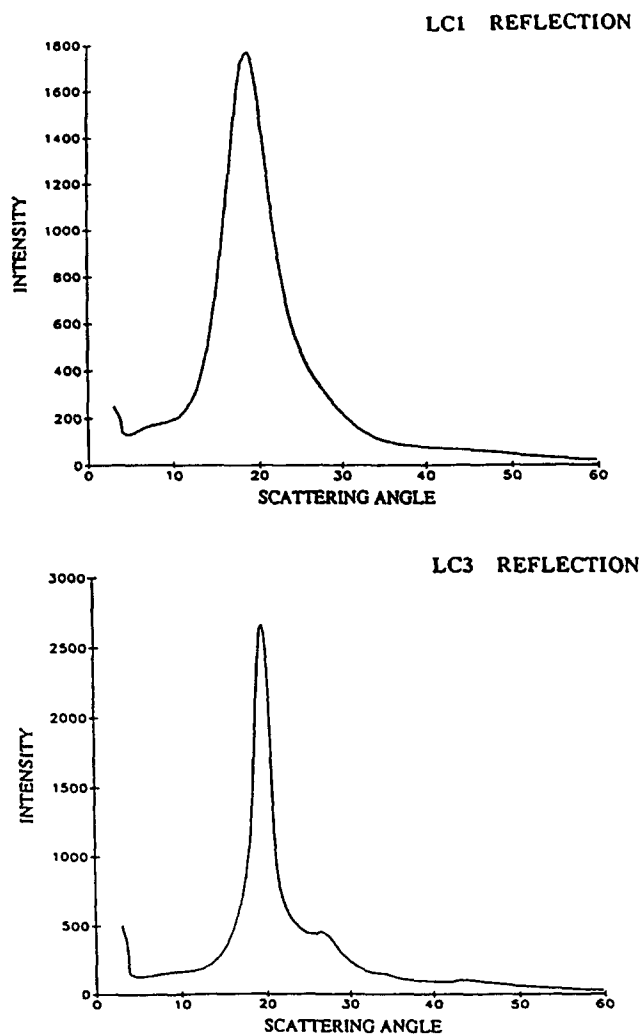


Figure 3 Wide angle X-ray diffractions scans for LC1 (top) and LC3 (bottom). LC1 is 'amorphous' while LC3 is semi-crystalline

idea that the groups with the highest rotational barriers, due to their more bulky side groups, have the highest  $T_g$ s.

Wide angle X-ray diffraction (WAXD) scans of the intensity versus  $2\theta$  for LC1 show a broad X-ray peak (Figure 3) at  $2\theta = 19^\circ$  and an extremely weak and broad peak at  $2\theta = 47^\circ$ . The  $19^\circ$  peak is the amorphous background and the lack of sharp diffraction peaks is characteristic of a polymer without significant three-dimensional crystalline order. While lack of sharp diffraction peaks rules out three-dimensional crystalline order, it does not rule out liquid crystalline order. WAXD data on LC3 show prominent crystalline diffraction peaks consistent with the d.s.c. detection of a melting endotherm (Figure 2). This behaviour is characteristic of higher crystalline order. LC2, 4, 5 and 7 have X-ray scans similar to that for LC1, indicating insignificant three-dimensional order.

All of the polymers in this series exhibit anisotropic behaviour above their flow temperature, evidenced by polarized optical hot-stage microscopy, which is characteristic of liquid crystalline behaviour. The polyesters that do not have discernible crystallinity, yet are liquid crystalline above the flow temperature, will be referred to as non-crystalline or 'amorphous' liquid crystalline polymers. These polymers have liquid crystalline order above the flow temperature that is essentially 'frozen-in' when cooled to temperatures

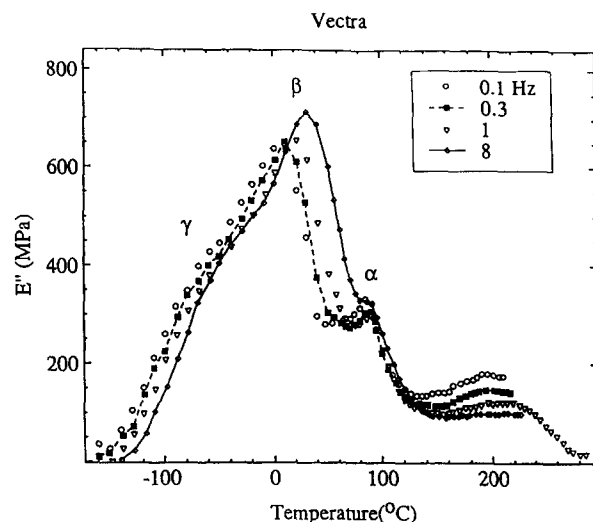


Figure 4 D.m.a. loss ( $E''$ ) data for Vectra<sup>®</sup> A950 at the four different frequencies indicated

below the glass transition temperature. The semi-crystalline LC polymers (LC3 and Vectra<sup>®</sup>) have both liquid crystalline order and three-dimensional crystalline order in the solid state.

#### D.m.a.

Frequency dependent d.m.a. studies are very important because of the complexity of the relaxations in these systems. Also, because some relaxations are stronger dielectrically than mechanically, one must be careful in interpretation. Frequency dependent d.m.a. spectra are shown in Figure 4 for Vectra<sup>®</sup> with the peaks assigned as  $\alpha$ ,  $\beta$ , and  $\gamma$  using the nomenclature of McCrum *et al.*<sup>26</sup>. The  $\alpha$  relaxation (glass transition) is best resolved at low frequencies by d.m.a. It is very weak dielectrically and is only observed at low frequencies<sup>20</sup>.  $\beta$  is attributed to the motion of the HNA group and  $\gamma$  to motions of the HBA group<sup>20</sup>.  $\gamma$  is very weak mechanically but very strong dielectrically and dominates the dielectric data, especially at high frequency<sup>20,22</sup>. The low activation energy of  $E_a = 17 \text{ kcal mol}^{-1}$  for  $\beta$  allows us to assign this as a local mode relaxation as was shown previously by low frequency a.c. dielectric data<sup>20</sup>.

Figure 6 shows  $E'$  at 1 Hz for both Vectra<sup>®</sup> and LC1. The  $\alpha$  relaxation is clearly the main glass transition in LC1, corresponding to the largest drop in  $E'$  (Figure 6). The modulus retains a larger value at the highest temperatures in Vectra<sup>®</sup> because of its crystallinity. Three relaxations are seen in the frequency dependent data for LC1 (Figure 5). Very high activation energies ( $E_a$ ) of 170 and 90  $\text{kcal mol}^{-1}$  are determined for the  $\alpha$  and  $\beta$  relaxations in LC1, respectively, indicating that they are both 'glass transitions'. The 'double  $T_g$ ' will be seen to be a common feature of several related LC polymers in this series. The low value of  $E_a = 17 \text{ kcal mol}^{-1}$  obtained from the data in Figure 5 for the  $\gamma$  relaxation in LC1 is consistent with the assignment of a local mode type of motion.

Mechanical loss data for LC1, LC2, LC3, and Vectra<sup>®</sup> are plotted in Figure 7 showing that the phenyl substitution on the hydroquinone group (LC2) leads to a lower 'main' glass transition than substitution of *t*-butyl (LC1), consistent with the d.s.c. data discussed

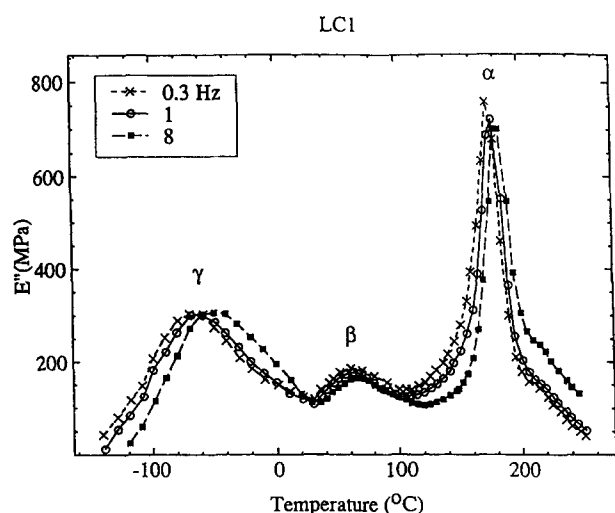


Figure 5 D.m.a. loss ( $E''$ ) data for LC1 at the three different frequencies indicated

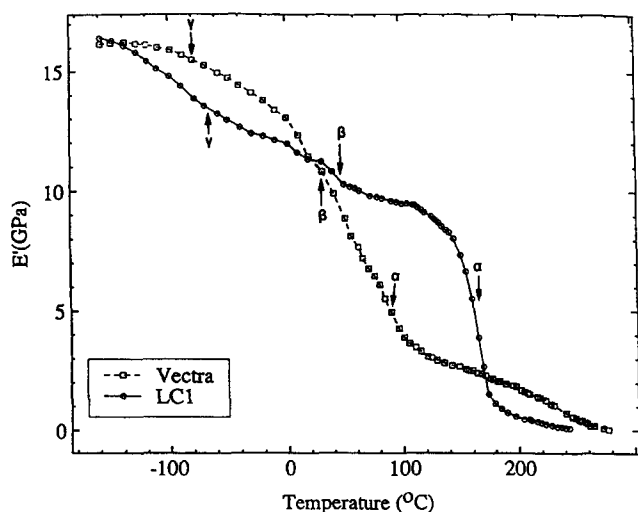


Figure 6 D.m.a. modulus ( $E'$ ) data for Vectra<sup>®</sup> and LC1 at 1 Hz

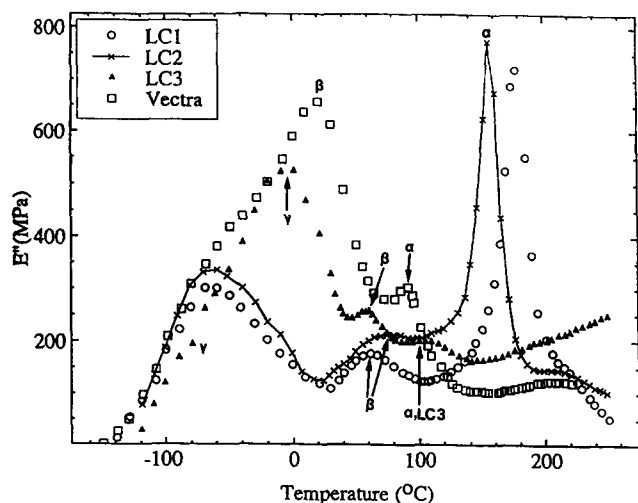


Figure 7  $E''$  versus temperature for the four LC polymers indicated. Three transitions are seen in each polymer and are designated from high to low temperatures as  $\alpha$ ,  $\beta$ , and  $\gamma$ , respectively (see text)

above (Figure 2). Very weak glass transition(s) are observed in LC3 where methyl hydroquinone was substituted for *t*-butyl hydroquinone. LC3 is semi-crystalline and the weak glass transition is seen at *ca* 105°C, and is referred to as an  $\alpha$  relaxation (Table 2). If a higher temperature relaxation (i.e. higher  $T_g$ ) is present in LC3, it is too weak and broad to be clearly resolved by any of the techniques applied here. We call both the 105°C ( $\alpha$ ) and 60°C ( $\beta$ ) relaxations 'glass transitions' because of their very high  $E_a$ s (Table 2). These activation energies are comparable to those obtained for the glass transition in semi-crystalline Vectra<sup>®</sup> A950<sup>20</sup>. These surprisingly low  $T_g$ s in the semi-crystalline Vectra<sup>®</sup> and LC3 samples presumably arise because of the low rotational barriers associated with the non-substituted, linear chain structures. Phenyl substitution (LC2) leads to significantly higher rotational barriers and *t*-butyl substitution (LC1) leads to even higher rotational barriers as can be seen by the variation in the d.m.a.  $T_g$ s (Figure 7, Table 2).

As was discussed above, the weak and narrow  $\beta$  relaxation in LC1 at 60°C is characterized by a very high activation energy as are the  $\beta$  relaxations for LC2 and LC3 at 75° and 60°C, respectively (Table 2). These values of  $E_a$  are much too high for secondary, local-mode relaxations and are good evidence that these are weak second glass transitions.

The  $\gamma$  relaxations in Figure 7 are very similar for LC1 and LC2 and occur at *ca* -65°C and are attributed to local motions of carbonyls adjacent to non-substituted aromatic groups such as HBA related species. For semi-crystalline LC3, the peak temperature of the intense  $\gamma$  relaxation is shifted about 60°C higher in temperature.

Figure 8 compares the control (LC1) with LC4, 5 and 7. In LC4, the biphenol is replaced by bisphenol A and the  $T_g$  remains unchanged indicating that rotational barriers are not significantly modified by the small amount of bisphenol A. The same can be said for LC5 where *t*-methyl biphenol is substituted for biphenol. Substitution with bisphenol A (LC4) leads to very similar  $\gamma$  and  $\beta$  relaxations compared to LC1, while substitution of *t*-methyl biphenol (LC5) leads to a splitting of the  $\gamma$  relaxation into a  $\gamma$  and a different broad and strong  $\beta$  relaxation. Unlike the case of the  $\beta$  relaxations around 60°C in LC1, 2, 3 and 4 which are assigned as second glass transitions, the  $\beta$  relaxation in LC5 is attributed to a local motion because of its large breadth and low activation energy (Table 2). The  $\gamma$  is likely a result of local motion of the HBA and related species, while the  $\beta$  is probably related to the more restricted local motions of the carbonyls near the *t*-methyl biphenol units. In LC7 the HBA is replaced by *t*-butyl substituted HBA leading to a slightly depressed  $T_g$  compared to LC1. The  $\gamma$  and  $\beta$  relaxations for LC7 and LC1 are very similar mechanically, even though dielectrically the magnitude of the  $\gamma$  relaxation is different for the two.

#### A.c. dielectric

Isochronal scans of the dielectric constant ( $\epsilon'$ ) and loss ( $\epsilon''$ ) for the control polymer, LC1, are shown in Figure 9. Two prominent relaxations are seen: a high temperature  $\alpha$  relaxation at 200°C (1 kHz) and a subglass ( $\gamma$ ) process occurring at -20°C (1 kHz). In addition, a weak  $\beta$  relaxation is seen at the lower frequencies and occurs at *ca* 110°C at 1 kHz. The activation energy of the

**Table 2** D.s.c. and d.m.a. relaxation summary<sup>a</sup> including activation energies ( $E_a$ )

Sample	Description	$T_g$ (d.s.c.)	$T_\alpha$	$T_\beta$	$T_\gamma$	$E_{a,\alpha}$	$E_{a,\beta}$	$E_{a,\gamma}$
LC1	t-BuHQ/BP/T/HBA	185	177	63	-66	170	90	17
LC2	Ph-HQ/BP/T/HBA	157	154	75	-66	136	50	14
LC3	Me-HQ/BP/T/HBA	—	105	60	-5	130 ± 20	150 ± 50	25
LC4	t-Bu-HQ/BPA/T/HBA	183	180	63	-67	180	—	14
LC5	t-Bu-HQ/t-Me-BP/T/HBA	185	179	24	-60	150	27	20
LC7	t-Bu-HQ/BP/T/t-Bu-HBA	172	162	64	-73	150	100 ± 30	15
Vectra <sup>®</sup>	HBA/HNA(73:27)	—	95	18	-60	120	30	12 <sup>b</sup>

<sup>a</sup> All relaxation temperatures (1 Hz) and activation energies were determined by d.m.a. unless otherwise indicated

<sup>b</sup>  $E_a = 12 \text{ kcal mol}^{-1}$  determined by dielectric<sup>20</sup>

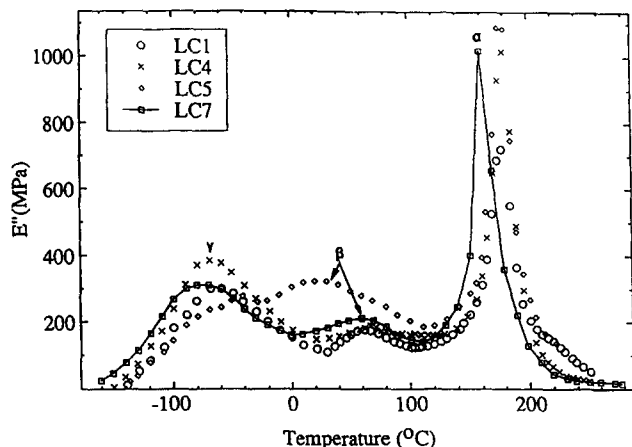


**Figure 8**  $E''$  versus temperature for the four LC polymers indicated

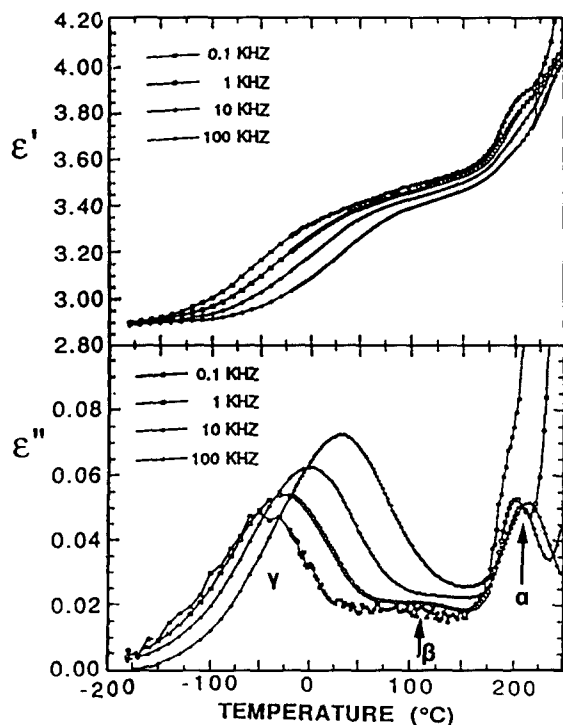


**Figure 9** Dielectric constant ( $\epsilon'$ ) (top) and loss ( $\epsilon''$ ) (bottom) versus temperature for LC1 (see text)

$\beta$  relaxation is difficult to obtain dielectrically because of the poorly defined peaks, but was shown by d.m.a. to be very large, characteristic of a glass transition. The main  $\alpha$  relaxation process in LC1 is relatively narrow,

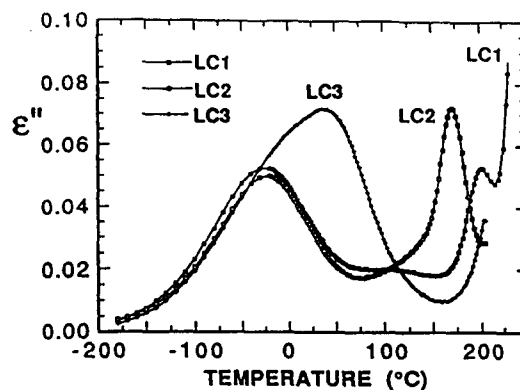


**Figure 10** Dielectric loss ( $\epsilon''$ ) versus temperature for the three polymers indicated (see text)

occurring over a range of approximately 30°C, while the subglass  $\gamma$  process is very broad extending over a wide temperature range of almost 200°C. The value of  $E_a$  for the  $\alpha$  relaxation is 180 kcal mol<sup>-1</sup> typical of a glass transition. At temperatures above  $T_g$ , the dielectric loss increases dramatically due to ionic conductivity, especially at low frequencies (Figure 9).

The effects of substituting side groups on the hydroquinone monomer are seen in isochronal  $\epsilon''$  (1 kHz) versus temperature scans for LC1, LC2, and LC3 (Figure 10). Substituting a phenyl group (LC2) or the t-butyl group (LC1) does not significantly affect the temperature or magnitude of the  $\gamma$  process, but increases the magnitude and lowers the temperature of the  $\alpha$  process. Substituting a methyl group for the t-butyl group leads to a semi-crystalline polymer (LC3) and a  $T_g$  (or  $\alpha$ ) relaxation which cannot be detected by dielectric methods. The  $\gamma$  process is shifted to higher temperatures for LC3.

A comparison of the isochronal dielectric  $\epsilon''$  (1 kHz) versus temperature for LC1, LC4, LC5 and LC7 is shown in Figure 11. Substituting bisphenol A (LC4) for 4,4'-biphenol does not significantly affect the relaxation processes. Incorporation of the tetramethyl biphenol (LC5) restricts the  $\gamma$  relaxation process in a kinetic sense, causing a clear separation of the low temperature relaxation into two broad relaxations, but has no significant effect on the  $\alpha$  process (Figure 11). Both the -30°C ( $\gamma$ ) and 100°C ( $\beta$ ) low temperature relaxations in LC5 are assigned as local non-cooperative relaxations because of their low activation energies (see Table 2 for values of  $E_a$  determined by d.m.a.).

Substituting t-butyl HBA (LC7) for HBA does not affect either the  $\alpha$  or  $\gamma$  process in a kinetic sense, but

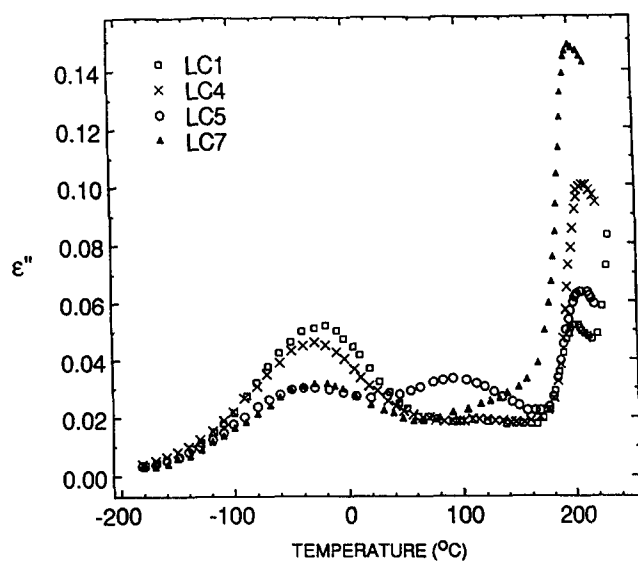


**Figure 11** Dielectric loss ( $\epsilon''$ ) versus temperature for the four polymers indicated (see text)

significantly affects the  $\gamma$  relaxation in a thermodynamic sense where it is seen that it is much weaker as compared to control LC1 (Figure 11). The lowered magnitude may arise because the esters related to the non-substituted aromatics (terephthalic acid plus biphenol) may be the only species capable of contributing to the dielectric  $\gamma$  relaxation in LC7 as will be discussed below.

## DISCUSSION

This series of liquid crystalline polymers exhibit three prominent relaxation processes. In most cases only two are detected by 1 kHz a.c. dielectric measurements so the discussion of the  $\beta$  relaxation below relies mainly on d.m.a. data. The high temperature ( $\alpha$ ) process is associated with the glass transition. The sub-glass ( $\gamma$ ) process is attributed to local main chain motions. The  $\beta$  relaxations are attributed to local mode relations in only two cases, Vectra<sup>®</sup> and LC5. The differences are discussed in detail below.

Dielectric studies of the glass transition in Vectra<sup>®</sup> and related materials are difficult because of the dominant  $\gamma$  relaxation and the moderately strong  $\beta$  relaxations which are due to local motions of the HBA and HNA related species, respectively<sup>20,22</sup>. Only at low frequencies can the very weak  $\alpha$  be separated from the  $\beta$  and  $\gamma$  dielectrically<sup>20</sup>. We have not studied Vectra<sup>®</sup> dielectrically, but in the low frequency d.m.a. data the  $\alpha$  relaxation is clearly separated from the  $\beta$  as expected<sup>20</sup> (Figure 4).

Mechanically, the shape, magnitude and activation energy of the  $\alpha$  relaxation in semi-crystalline LC3 at 105°C (Figure 7) are very similar to the  $\alpha$  relaxation in semi-crystalline Vectra<sup>®</sup> A950 (Figure 4), i.e. they are all sharp and relatively weak<sup>18,23</sup>. No  $\alpha$  relaxation is detected in LC3 dielectrically at the frequencies that we have used. These surprisingly low  $T_g$ s in the semi-crystalline Vectra<sup>®</sup> and LC3 samples presumably arise because of the low rotational barriers associated with the linear non-substituted aromatic main chain structures. Phenyl substitution (LC2) of the hydroquinone units leads to significantly higher rotational barriers and t-butyl

substitution (LC1) leads to even higher rotational barriers as can be seen by the mechanical glass transitions ( $\alpha$ ) increasing in the order LC1 > LC2 > LC3 (Figure 7, Table 2).

We were rather surprised at the presence of the sharp and narrow  $\beta$  relaxations between 60° and 75°C in the d.m.a. data of LC1, 2, 3, 4 and 7 (Figures 7 and 8). They are all characterized by very high activation energies of the order of 50–150 kcal mol<sup>-1</sup> (Table 2). These values are much too high for secondary, local-mode relaxations and are good evidence that these are weak second glass transitions. A likely source of these weak glass transitions at such low temperatures, are backbone cooperative motions due to units other than the substituted hydroquinones, such as HBA related segments. These unsubstituted aromatic species would lead to relatively low rotational barriers to rotation. This also would explain the rather low  $T_g$  in Vectra<sup>®</sup> which consists entirely of unsubstituted aromatic esters. In LCPs, these barriers are even lower than they would be with isotropic polymers, because in the 'liquid crystalline' glassy state the chains are somewhat parallel to each other. This has been shown experimentally in several cases where the same polymer could be quenched into either an isotropic or an anisotropic glass<sup>25,27</sup>.

Regarding these high activation energy  $\beta$  relaxations with glass transition-like properties, it is likely that HBA rich blocks and related chain segments would have to be present to give rise to units large enough to have their own separate glass transition. Chemical heterogeneity of copolyesters leading to non-randomness or blockiness has been addressed in many studies<sup>28,29</sup> including studies of broadened glass transitions<sup>25</sup>.

The  $\alpha$  relaxation in LC3 is also similar in activation energy (Table 2), shape, and intensity, to these other glass transition-like  $\beta$  relaxations (Figure 7) and to the Vectra<sup>®</sup> glass transition (Figure 4). The  $\alpha$  relaxation in LC3 is also likely attributable to glass transition like motions associated with the non-crystalline chain components of the methyl substituted hydroquinone units, while the  $\beta$  in LC3 at slightly lower temperature is likely attributed to the non-substituted aromatic esters.

Turning to the lowest temperature relaxations, the  $\gamma$  relaxations in LC1, 2, and 4 are all quite similar by d.m.a. (Figures 7 and 8) and dielectric methods (Figures 10 and 11). The  $\gamma$  relaxation is shifted to higher temperatures in LC3, separates into two transitions in LC5, and is weakened in LC7. To explain some of these features, it is noted that all polymers except LC7 have large fractions of unsubstituted aromatic ester groups giving rise to the classical -60°C (1 Hz)  $\gamma$  relaxation, seen also in Vectra<sup>®</sup> like polymers at about this temperature<sup>20</sup>. Except in the case of LC7, the  $\gamma$  relaxation is in large part due to the high HBA content of the polymers studied here. Even LC7 has a finite fraction of unsubstituted aromatic esters because of the linkages of terephthalic acid with biphenol. This lower fraction in LC7 is probably why the  $\gamma$  relaxation is smaller dielectrically as compared to LC1–LC4 (Figures 10 and 11).

The  $\gamma$  relaxation in LC3 is shifted upward in temperature compared to the control polymer, LC1. This is due to changes in chemical structure and probably not due to crystallinity. For example, in non-LC polymers such as poly(ethylene terephthalate), the

presence of crystallinity has no effect on the location of the local mode relaxation but shifts the glass transition to higher temperatures<sup>26</sup>. The low temperature side of the  $\gamma$  transition in LC3 is very similar to those of LC1 and LC2 (Figure 10) indicating that there are possibly overlapping relaxations due to different chain units contributing to the broadened transition in LC3. The  $\gamma$  relaxation in LC1 and LC2 and the low temperature side of the  $\gamma$  relaxation in LC3 are presumably attributed to the more mobile unsubstituted aromatic esters such as HBA, while the higher temperature part of the  $\gamma$  in LC3 is due to the more kinetically constrained methyl substituted hydroquinone. This could be attributed to better chain packing and more steric hindrance in LC3 because of the smaller size of the methyl group in the substituted hydroquinone. It is possible that the  $\gamma$  relaxation in LC1 and LC2 are essentially the same, because only the higher mobility, unsubstituted aromatic esters can contribute to this relaxation. Presumably, contributions of t-butyl (LC1) and phenyl (LC2) substituted groups result in sub-glass motions which are too weak or broad to be detected because of their higher steric hindrance. LC4 also has essentially the same  $\gamma$  relaxation as LC1 and LC2, and for a similar reason, the  $\gamma$  relaxation in LC4 is not affected by substitution of the bisphenol-A group.

In LC5, the  $\gamma$  relaxation separates into two clear but broad local mode relaxations (Figures 8 and 11). The higher temperature local mode relaxation ( $\beta$ ) is presumably due to the methyl side groups at the *ortho* position of the ester linkage of the tetramethyl biphenol monomer. This behaviour is similar to the behaviour observed in polyarylates and polycarbonates<sup>26,30</sup> where *ortho*-substitution on the biphenol or BPA group adjacent to the ester linkage shifts the subglass process to much higher temperatures. Since the biphenol accounts for only 20 mol% of the total diol, two subglass processes are present. As was discussed above, the lower temperature local mode relaxation ( $\gamma$ ) in LC5 is attributed to motion of unsubstituted aromatic esters, and is also seen for the control polymer (LC1) except that there are more unsubstituted species in LC1 so the  $\gamma$  relaxation is stronger (Figure 11).

## REFERENCES

- 1 Roviello, A. and Sirigu, A. J. *J. Polym. Sci., Polym. Lett. Ed.* 1975 **13**, 455
- 2 Jackson, W. J. and Kuhfuss, H. *J. Polym. Sci., Polym. Chem. Ed.* 1976, **14**, 2043
- 3 Jackson, W. J. Jr. *Br. Polym. J.* 1980, **12**, 154
- 4 Griffin, B. P. and Cox, M. K. *Br. Polym. J.* 1980, **12**, 147
- 5 Calundann, G. W. and Jaffe, M. 'Proc. Robert A. Welch Foundation. Conf. Res. XXVI', 1982
- 6 Economy, J. *J. Macromol. Sci. - Chem.* 1984, **A21**, 1705
- 7 Jackson, W. J. Jr., *J. Appl. Polym. Sci., Appl. Polym. Symp.* 1985, **41**, 25
- 8 Chung, T.-S. *Polym. Eng. Sci.* 1986, **26**, 901
- 9 Connolly, M. S. (DuPont). U. S. Patent 4664972, 1987
- 10 Connolly, M. S. (DuPont). U. S. Patent 4746566, 1988
- 11 Kwolek, S. L., Morgan, P. W. and Schaeffgen, J. R. 'Encyclopedia of Polymer Science and Technology', Vol. 9, John Wiley, New York, 1985, p. 1
- 12 Frosini, V., De Petris, S., Chiellini, E., Galli, G. and Lenz, R. *Mol. Cryst. Liq. Cryst.*, 1983, **98**, 223
- 13 Gedde, U. W., Buerger, D. and Boyd, R. H. *Macromolecules* 1987, **20**, 988
- 14 Wendorff, J. H., Finkelmann, J. and Ringsdorf, H. *J. Polym. Sci., Polym. Symp.* 1978, **63**, 245
- 15 Zentel, R., Strobl, G. R. and Ringsdorf, H. *Macromolecules* 1987, **18**, 960
- 16 Kresse, H. and Shibaev, V. P. *Macromol. Chem., Rapid Commun.* 1984, **5**, 63
- 17 Clements, J., Davies, G. R., Jakeways, R., Troughton, M. J. and Ward, I. M. *Polym. Mater. Sci. Eng.* 1985, **52**, 8
- 18 Blundell, D. J. and Buckingham, K. A. *Polymer* 1985, **26**, 1623
- 19 MacDonald, W. A. *Mol. Cryst. Liq. Cryst.* 1987, **153**, 311
- 20 Alhaj-Mohammed, M. H., Davies, G. R., Abdul Jawad, S. and Ward, I. M. *J. Polym. Sci., Polym. Phys. Ed.* 1988, **26**, 1751
- 21 Brostow, W. *Polymer* 1990, **31**, 979
- 22 Kalika, D. S. and Yoon, D. Y. *Macromolecules* 1991, **24**, 3404
- 23 Turek, D. E. and Simon, G. P. *Polym. Int.* 1992, **27**, 165
- 24 Zhang, H., Davies, G. R. and Ward, I. M. *Polymer* 1992, **33**, 2651
- 25 Sauer, B. B., Beckerbauer, R. and Wang, L. *J. Polym. Sci., Polym. Phys. Ed.* 1993, **31**, 1861
- 26 McCrum, N. G., Read, B. E. and Williams, G. 'Anelastic and Dielectric Effects in Polymeric Solids', Wiley, London, 1967, republished Dover, New York, 1991
- 27 Chen, D. and Zachmann, H. G. *Polymer* 1991, **32**, 1613
- 28 Lenz, R. W. and Feichtinger, K. A. *Am. Chem. Soc. Polym. Prepr.*, 1979, **20**, 114
- 29 MacDonald, W. A., McLenaghan, A. D. W., McLean, G., Richards, R. W. and King, S. M. *Macromolecules* 1991, **24**, 6164
- 30 Illers, K. H. and Breuer, H. *J. Colloid Sci.* 1963, **18**, 1